

Contents

1	Overview	1
2	Theoretical model	5
3	Small sampling effects	7
4	Finite size effects	8
5	Packing fraction effects	9
6	Next-nearest-neighbor and nonlinear effects	10
7	Topological properties of defects	11

1 Overview

This document is meant to log my progress in the investigation of mechanical modes in crystals of hard regular polygon particles. The system consists of $N = n^2 \times n_{\text{unit}}$ particles, where n is some integer and n_{unit} is the number of particles in the unit cell. The system is initialized in its densest known packing and then the crystal vectors are enlarged by constant factors to achieve a prescribed packing fraction. The motion of particles is decomposed into $n \times n$ distinct Fourier modes. There are $3n_{\text{unit}}$ relevant fields to investigate. The first $2n_{\text{unit}}$ are phonon fields signified by $\tilde{\mathbf{u}} = (\tilde{u}_x, \tilde{u}_y)$ (if the number of particles per unit cell is greater than 1, then these fields are further indexed *i.e.* $\tilde{\mathbf{u}}^{\alpha, \beta, \gamma \dots}$). The remaining n_{unit} fields are libron fields, signified by $\tilde{\theta}^{\alpha, \beta, \gamma \dots}$. In the case of hexagons, $n_{\text{unit}} = 1$, and in the case of many other polygons including pentagons studied here, $n_{\text{unit}} = 2$.

The various control parameters in a simulation are n the number of unit cells along one side of the box, ϕ the packing fraction, s the number of simulation steps, and the polygon shape. The densest packing, and thus the crystal lattice vectors, are determined by the polygon. The real space lattice vectors given by $\mathbf{a}_1, \mathbf{a}_2$ are usually meant to be in the densest packing, ϕ_{max} . When the system is relaxed to a smaller packing fraction, the lattice vectors are presumed to be $\mathbf{a}_i(\phi) = \mathbf{a}_i \sqrt{\phi_{\text{max}}/\phi}$. The reciprocal lattice vectors \mathbf{G}_i are constructed from these real space lattice vectors, and the unit cell of the reciprocal lattice forms the Brillouin zone within which \mathbf{k} vectors are sampled. The relevant \mathbf{k} vectors to sample are $n_1 \mathbf{G}_1/n + n_2 \mathbf{G}_2/n$, where n_i are integers. This way, the same number of Fourier modes are sampled as there are degrees of freedom in the real space system.

The Fourier modes are analyzed by considering their correlation functions. In Monte Carlo, dynamical information is not available, so collective degrees of freedom need to be analyzed from

correlation functions by way of a kind of generalized law of equipartition. We assume that this hard particle system which is controlled exclusively by entropic interactions can be approximated by a harmonic Hamiltonian:

$$\mathcal{H} = \frac{1}{2m} p_i \delta_{ij} p_j + \frac{1}{2I} L_i \delta_{ij} L_j + \frac{1}{2} x_i K_{ij} x_j. \quad (1)$$

The first term is the translational kinetic energy and the second term is the rotational kinetic energy. The last term is a harmonic coupling by a $3N \times 3N$ matrix, and x_i represent both the particle positions and particle orientations. In thermal equilibrium, it is provable that

$$\langle x_i x_j \rangle = k_B T K_{ij}^{-1}. \quad (2)$$

The matrix K_{ij} is partially diagonalized by the Fourier transform with respect to the lattice vectors $\mathbf{a}_{1,2}(\phi)$, so we find that

$$\langle \tilde{x}_{\mu,\mathbf{k}}^* \tilde{x}_{\nu,\mathbf{k}} \rangle = C_{\mu\nu,\mathbf{k}} = k_B T K_{\mu\nu,\mathbf{k}}^{-1}. \quad (3)$$

This decomposes the large $3N \times 3N$ matrix K_{ij} into a block diagonal $n^2 \times n^2$ matrix whose diagonal elements are $3n_{\text{unit}} \times 3n_{\text{unit}}$ matrices $K_{\mu\nu}$. The modes \tilde{x}_μ can represent either $\tilde{\mathbf{u}}_x^{\alpha,\beta\cdots}$, $\tilde{\mathbf{u}}_y^{\alpha,\beta\cdots}$ or $\tilde{\theta}^{\alpha,\beta\cdots}$. The ultimate output of the analysis are the $K_{\mu\nu,\mathbf{k}}$, which are obtained by computing every correlation function of all modes of the same wave vector and inverting the resulting matrix $C_{\mu\nu,\mathbf{k}}$. The elements of $\mathbf{K}_{\mathbf{k}}$ are the squares of the phonon and libron dispersion relations, *i.e.* they furnish $\omega^2(\mathbf{k})$ for all \mathbf{k} sampled in the Brillouin zone and for all collective modes $\tilde{\mathbf{u}}^{\alpha,\beta\cdots}$ and $\tilde{\theta}^{\alpha,\beta\cdots}$.

The matrices $\mathbf{K}_{\mathbf{k}}$ depend on the packing fraction ϕ , the number of particles N , and the number of Monte Carlo sweeps taken s . If s is too small, then there is not a sufficient number of statistically independent Monte Carlo frames to compute the elements of the correlation matrix \mathbf{C} . The effect of s will be explored in Section 3.

In principle, the matrix \mathbf{C} should be independent of N (or equivalently n), but having larger N helps resolve \mathbf{C} as a function of \mathbf{k} , the wavevector, as the Brillouin zone is more densely populated. The effect of N will be explored in Section 4.

The matrix \mathbf{C} is most markedly affected by changes in the packing fraction. Because polygon crystals melt into various phases (hexatic, rotator, or plain fluid), particular elements of \mathbf{C} should simply vanish across these transitions, which I will show leads to flat dispersion relations. That is, particular elements of $\mathbf{K}_{\mathbf{k}}$ become independent of \mathbf{k} . The effect of packing fraction will be shown in Section 5.

One of the difficulties in discerning meaningful interpretations of $\mathbf{K}_{\mathbf{k}}$ is obviously the high dimensionality of the matrix. It is necessarily symmetric, so it has $3n_{\text{unit}}(3n_{\text{unit}} + 1)/2$ independent components, each of which is a function of the two-dimensional \mathbf{k} . Even for the one-particle unit cell of the hexagon crystal, there are 6 independent elements of $\mathbf{K}_{\mathbf{k}}$ that need to be explored. Luckily, at quadratic order, the phonon mode is uncoupled from the libron mode, so this reduces the 6 components to 4 components (this uncoupling will also be demonstrated explicitly in Section 6).

To alleviate the difficulty in plotting a large-dimensional object as a function of a two-dimensional object, I resorted to taking cross sections in the Brillouin zone and plotting each of the $3n_{\text{unit}}(3n_{\text{unit}}+1)/2$ elements in the same figure. A sample plot is shown in Figure 1. These should be interpreted as giving the square frequencies of collective modes.

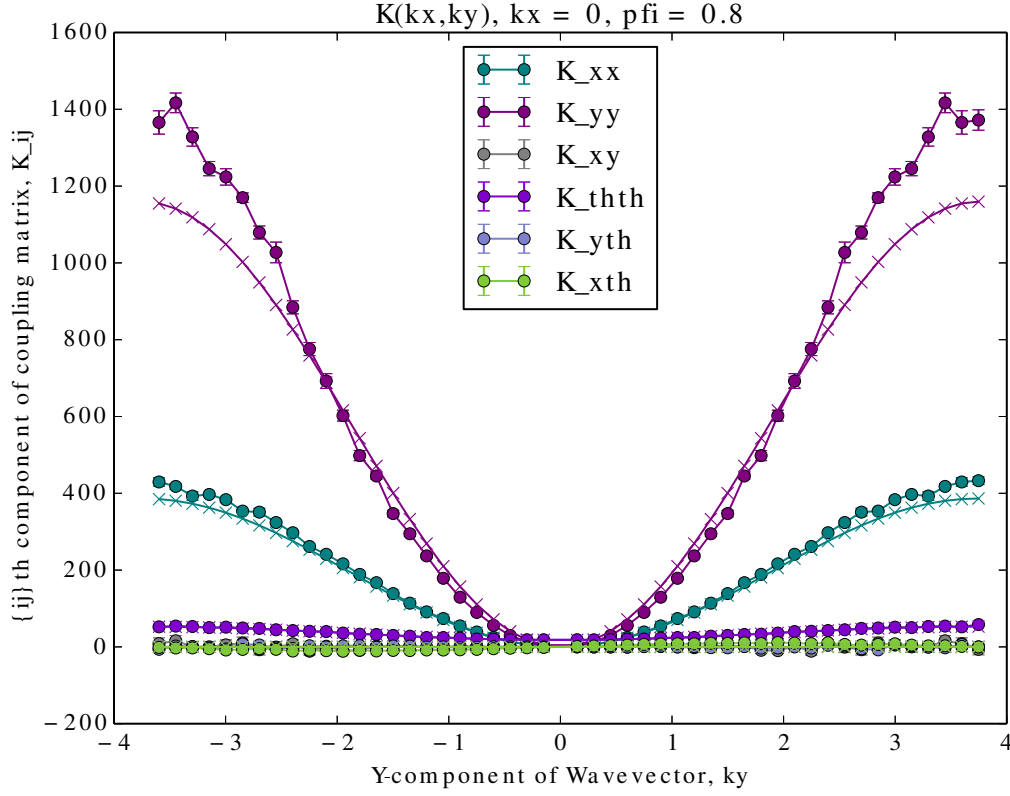


Figure 1: Sample figure for $\phi = 0.8$ (I used “pfi” for “packing fraction” and don’t remember why I had the extra i). The curves marked with closed circles and error bars are from simulation data, and curves of the same color marked with x’s are best-fit theoretical curves. The object K_{yy} is the dispersion curve for a longitudinal phonon traveling in the y direction (because here, the component $k_x = 0$), and K_{xx} is the dispersion for a transverse phonon. Along this particular axis in the Brillouin zone, the off-diagonal component K_{xy} is 0, but is displayed anyway. $K_{\theta\theta}$ is the dispersion for the libron, and because it is so much smaller than the phonon dispersion, we see that the libron is a more relaxed mode than the phonon. The off-diagonal elements $K_{x\theta}$ and $K_{y\theta}$ should also be 0 for all points in the Brillouin zone, but are also shown anyway. More plots will feature the θ elements zoomed in.

2 Theoretical model

The dispersion curves produced by the Fourier analysis described in Section 1 are fitted by a harmonic lattice model. A fundamental assumption of all the models is that the free energy of the system can be broken down into a sum of pairwise potentials between polygons that are close together. The simplest model assumes that this effective interaction energy is so close range that only nearest neighbors of the lattice feel each other. Furthermore, the two-body interaction potential is assumed to be at least twice-differentiable, so a harmonic approximation can be made. With the quadratic assumption, the dispersion curves can be calculated exactly as a function of only a couple parameters which correspond to second derivatives of the two-body potential. Lattices with high symmetry like the triangular lattice of hard hexagons have only 3 free parameters (1 for the phonons and 2 for the librations). In general, the theoretical matrix $\mathbf{K}_{\mathbf{k}}$ is of the form

$$\mathbf{K}_{\mathbf{k}} = \begin{pmatrix} K_{xx} & K_{xy} & K_{x\theta} \\ K_{xy} & K_{yy} & K_{y\theta} \\ K_{x\theta} & K_{y\theta} & K_{\theta\theta} \end{pmatrix} = \begin{pmatrix} 4\gamma_{xx} & 4\gamma_{xy} & 0 \\ 4\gamma_{xy} & 4\gamma_{yy} & 0 \\ 0 & 0 & 4\mu + 4\gamma \end{pmatrix}. \quad (4)$$

$$\gamma_{ij} = \frac{1}{2} \sum_{\mathbf{c}} A_{\mathbf{c}} \hat{c}_i \hat{c}_j \sin^2 \left(\frac{\mathbf{k} \cdot \mathbf{c}}{2} \right), \quad \gamma = \frac{1}{2} \sum_{\mathbf{c}} E_{\mathbf{c}} \sin^2 \left(\frac{\mathbf{k} \cdot \mathbf{c}}{2} \right), \quad \mu = \frac{1}{2} \sum_{\mathbf{c}} D_{\mathbf{c}} \cos^2 \left(\frac{\mathbf{k} \cdot \mathbf{c}}{2} \right). \quad (5)$$

The off-diagonal elements used to contain parameters like B , C , and F , but those ended up going to zero by symmetries, so I found myself in a similar boat to Maxwell, who had so many vector fields to deal with while formalizing electromagnetic theory that he just labeled them alphabetically. The constants $A_{\mathbf{c}}$, $E_{\mathbf{c}}$ and $D_{\mathbf{c}}$ depend on the vector \mathbf{c} which separates two particles. In the hexagon lattice, all the nearest neighbors are the same by six-fold symmetry, so all of these parameters are independent of \mathbf{c} . In the pentagon lattice, the crystal only has two-fold symmetry, which brings us from 18 independent parameters to 9.

If we include next nearest neighbor interactions, then this introduces another set of constants that correspond to a second derivative of the effective interatomic pair potential, this time at a further distance. For both hexagons and pentagons, this would double the number of phenomenological constants to fit to. However, all of these constants appear as exterior multiplicative factors: the functional form of the dispersion curves are entirely predicted.

N s ϕ	0.850	0.800	0.750	0.710	0.700	0.690	0.680
$26^2, 3 \times 10^6$	✓	✓	✓	✓	✓	✓	✓
$50^2, 3 \times 10^6$	×	×	×	×	×	×	×
$100^2, 3 \times 10^6$	×	×	×	×	×	×	×
$26^2, 1 \times 10^7$	✓	r	r	r	r	r	r
$50^2, 1 \times 10^7$	✓	✓	✓	✓	✓	✓	✓
$100^2, 1 \times 10^7$	×	✓	✓	✓	✓	✓	✓
$26^2, 3 \times 10^7$	✓	?	?	?	?	?	?
$50^2, 3 \times 10^7$	×	×	×	×	×	×	×
$100^2, 3 \times 10^7$	×	×	×	×	×	×	×

3 Small sampling effects

In a given simulation, s is the number of Monte Carlo sweeps, and snapshots are taken at a period such that there are 10^3 presumably statistically independent frames to make correlation functions from. Therefore, every sampled frame is separated a period of $T = s \times 10^{-3}$ sweeps. If this period is too small, frames won't be sufficiently independent from each other and spurious correlations will be introduced. However, if T is needlessly long, simulation time is wasted. Below are some plots of the dispersion curves at various packing fractions for hexagons. Keep in mind that at around $\phi = 0.700\text{--}0.710$ the crystal melts into a hexatic phase. It's not unreasonable that critical slowing down may occur near this transition point, and so shorter simulations may vary from longer simulations significantly.

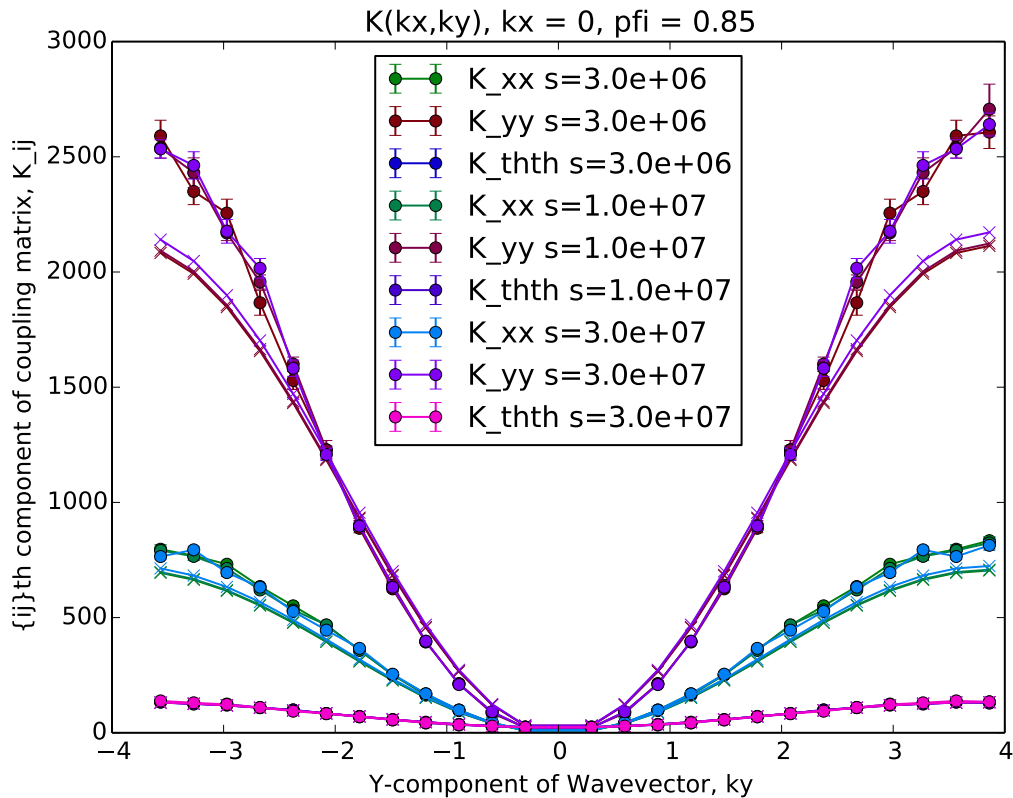


Figure 2: $N = 676$ and $\phi = 0.850$. For a sufficiently dense crystal, running the simulation longer than 3×10^6 sweeps doesn't change the dispersion curves at all.

4 Finite size effects

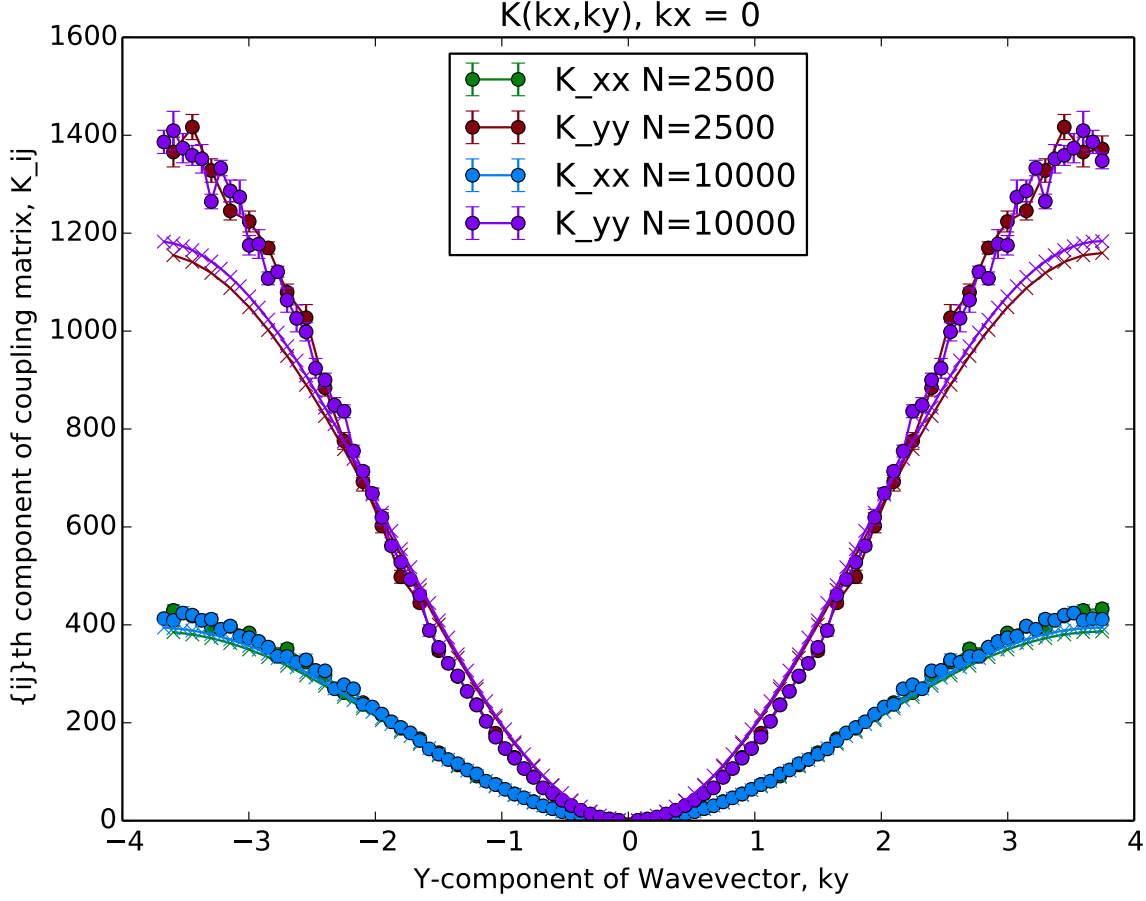


Figure 3: Phonon dispersion for two systems at $\phi = 0.8$, one has $N = 50^2$ and the other has $N = 100^2$. The simulation data are essentially identical, and the theoretical curves vary by about 2%. The $N = 100^2$ curve has the advantage of having finer resolution in k -space, but the $N = 50^2$ curve takes far less time to run. The theoretical curves show striking systematic error for large values of k_y

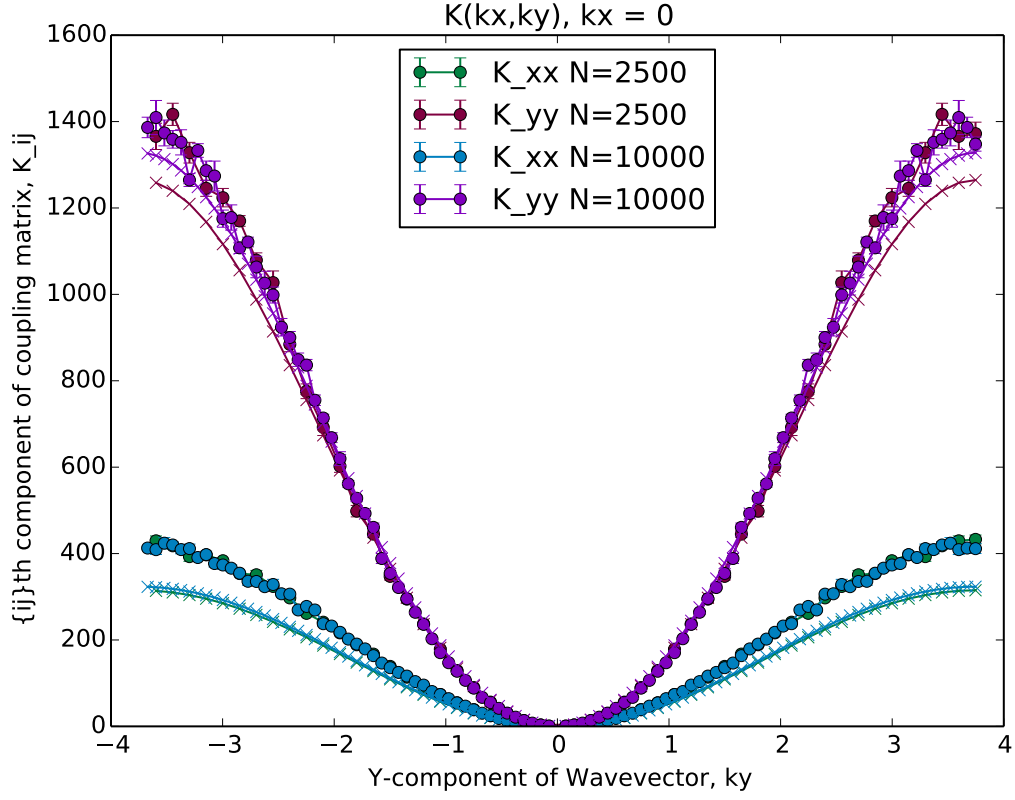


Figure 4: Same systems as Figure 3, but now the theoretical curves include next-nearest-neighbor interactions. By including these interactions, the fitting model gains another parameter, an effective next-nearest-neighbor stiffness constant. This model fits the longitudinal phonon curve better, but not the transverse anymore.

5 Packing fraction effects

6 Next-nearest-neighbor and nonlinear effects

7 Topological properties of defects